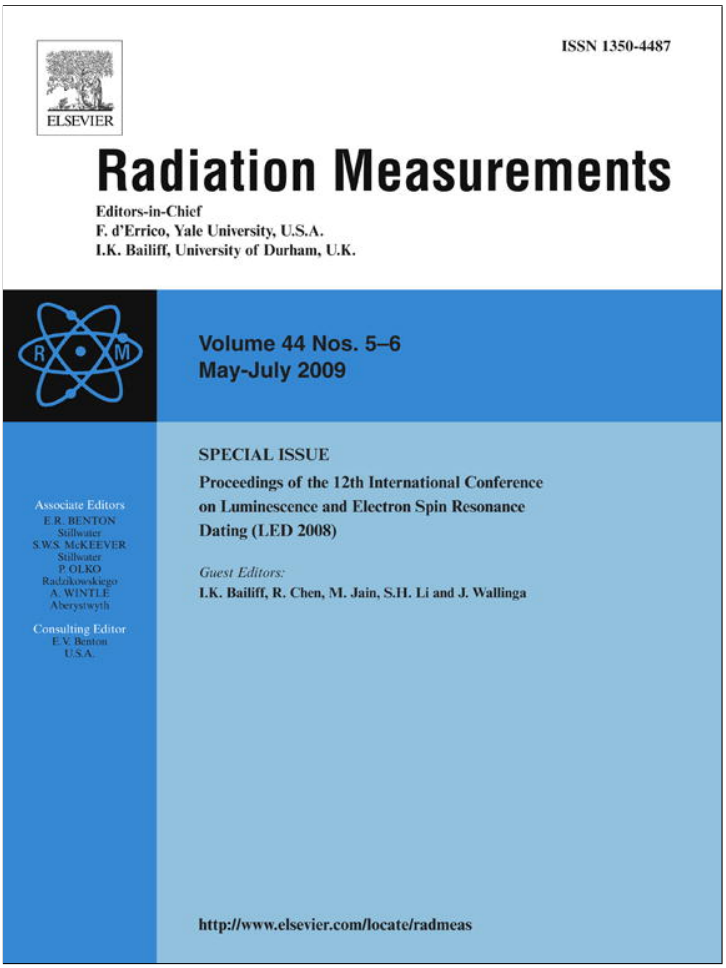

Radiation Measurements 44 (2009) 494–500

Contents lists available at ScienceDirect

Radiation Measurements

journal homepage: www.elsevier.com/locate/radmeas

Internal α activity: localisation, compositional associations and effects on OSL signals in quartz approaching β saturation

C.I. Burbidge [a,*], M.I. Dias [a], M.I. Prudêncio [a], L.P. Rebêlo [b], G. Cardoso [a], P. Brito [b]

[a] Instituto Tecnológico e Nuclear, Sacavém, Portugal
[b] DGM, INETI, Departamento de Geologia Marinha, Alfragide, Portugal

ARTICLE INFO

Article history:
Received 19 October 2008
Received in revised form
18 March 2009
Accepted 11 June 2009

Keywords:
Luminescence
Component
Dose response
Dose rate
Alpha
Internal
Impurity
Inclusion
Defect

ABSTRACT

Luminescence signals from hydrofluoric acid etched grains of quartz from Mozambican dunes were investigated in terms of elemental impurities, structural defects, and their relationship to internal α activity, to examine the potential for this to cause differences in signal levels obtainable from natural and laboratory irradiated samples. Optical and scanning electron microscopy (SEM), X-ray fluorescence (XRF) and instrumental neutron activation analysis (INAA) indicated the presence of various types of quartz and mineralogical inclusions. A spatial association of Th and U with Fe in structural defects was observed. Fe concentrations and inclusion sizes indicated that internal α dose rate would affect the defects that contained these impurities, but would be insignificant to the bulk quartz.

A broad range of optically sensitive thermoluminescence (TL) peaks were observed from this material, and indicated a preheating regime of 260 °C for 30 s to minimise effects of the observed inclusions and defects on absorbed dose determinations by optically stimulated luminescence (OSL). Growth in OSL with dose from etched coarse grains preheated in this way approached saturation by 332 Gy of β irradiation (^{90}Sr/^{90}Y) and by 4 kGy of α irradiation ($E \approx 3.5$ MeV: approximate natural soil spectrum average, using converted dose rate from ^{241}Am). This indicated α-efficiency (k_{eff}) at saturation of less than 0.08. However, the OSL decay curves contained a small 'medium' component. Structural defects introduced by milling the grains produced a larger 'medium' component with a similar decay rate under optical stimulation, which exhibited high saturation doses (>32 kGyα, >8.4 kGyβ) and α-efficiency ($k_{eff} = 0.34$). Maximum dose normalised OSL signals from the milled material greatly exceeded those obtainable from the whole etched grains.

It is inferred that the presence of structural defects within a quartz crystal, similar to those produced by milling, can produce OSL components that grow to signal levels and doses exceeding those from the crystalline quartz. In the present study such defects were found to host α-emitting impurities. High localised dose rates in nature could enhance signals from these locations without affecting the bulk crystal, producing high natural signal levels that may be difficult to reproduce in the laboratory. Association of internal α activity with Fe indicates potential for removal of the most α affected grains by magnetic separation. With or without associated α activity, signals from such defects may contribute to observed variability in the dose response of quartz OSL.

1. Introduction

Optically stimulated luminescence (OSL) dating is being applied to understand the formation of the Mozambican coastal plain. Quartz separates from old dune sands in this region have yielded natural OSL signals higher than those attainable by continuous β irradiation in the laboratory (Armitage, 2003; Armitage et al., 2006). Investigation of trapping competition effects show that staged irradiation of such samples, with charge transfer by heating in between, can increase the saturation intensity of β-induced signals by ~10% (Bailey et al., 2005). However, natural quartz often contains impurities such as Al, Ti and Fe, inclusions such as titanite, zircon, and dumortierite (Kibar et al., 2007), and voids that may contain water (Miallier et al., 2001). Quartz with large numbers of

* Corresponding author. Grupo de Geoquimica Aplicada & Luminescencia no Patrimonio Cultural, Instituto Tecnologico e Nuclear, Estrada Nacional 10, 2686-953, Sacavém, Portugal. Tel.: +351 219 994 6000; fax: +351 219 994 6185.
E-mail address: christoph@itn.pt (C.I. Burbidge).

1350-4487/$ – see front matter © 2009 Published by Elsevier Ltd.
doi:10.1016/j.radmeas.2009.06.007

structural defects (e.g. quartzite, flint) may exhibit broad TL curves and strong signal growth into the kGy region. TL of pre-irradiated flint has also been observed to respond to additional α irradiation, when additional β irradiation produced little effect (Mercier et al., 1992). Zircon displays some similar TL characteristics, including peaks commonly around 180 and 250 °C (Aitken, 1985a; Krbetschek et al., 1997). Such inclusions and defects may incorporate U and Th, which would provide an internal α dose rate to the quartz and the inclusion. Competition effects are likely to differ between α and β radiation on account of localised energy deposition by α particles (Zimmerman, 1972).

The present study focuses on quartz grains, isolated using density separation and treatment with concentrated hydrofluoric acid, from 34 samples taken from dunes of the Mozambican coast in 2005. It examines the hypothesis that localised α-emitting impurities within the grains, and the luminescence behaviour of defects hosting them, could produce differences between the natural luminescence response and that regenerated in the laboratory using β irradiation. A series of measurements were made with the objectives of evaluating:

(i) Average impurity concentrations and the composition of localised inclusions, in grains of quartz prepared for luminescence dating from bulk sediment.
(ii) TL and OSL signals contributing to the ~380 nm emission from these grains.
(iii) The potential of α radiation to induce additional OSL signal beyond that produced by β irradiation, in both compact crystalline quartz (the surfaces of acid etched grains), and in milled quartz with large numbers of defects exposed on grain surfaces.

2. Methods

Samples were prepared using the following sequence: dry sieve 160–250 μm; H_2O_2; HCl; 40% HF for 40 min (1st); HCl; density separation 2.62–2.70 gcm^{-3}; 40% HF for 40 min (2nd), HCl; resieve 160 μm. For luminescence measurements the grains were deposited in monolayers on stainless steel cups using silicone oil for adhesion. Subsamples of the prepared grains were inspected using an optical microscope. Other subsamples were powdered using a rotary mill, with low impurity Al_2O_3 grinding pieces to minimise contamination of the quartz, and 200 mg each were removed for instrumental neutron activation analysis (INAA; Al was not tested for). From the remainder, the 4–11 μm fraction was separated using Stokes settling in acetone (2–20 min, 7 cm column), and these grains were settled in monolayers onto aluminium disks for luminescence measurements.

Luminescence measurement and β irradiation were made using a Risø DA-15 automatic reader: OSL, 470 nm LED; TL, 0–500 °C; 5 °C s^{-1}, 7.5 mm Hoya U-340 detection filter, ^{90}Sr/^{90}Y irradiator (Bøtter-Jensen et al., 2000) giving 0.083 Gy s^{-1} to coarse grains on steel cups and 0.066 Gy s^{-1} to fine grains on aluminium disks (decay corrected from Richter et al., 2003). A Littlemore 6-source ^{241}Am unit with 'tall pillars' was used for α irradiation: decay corrected average strength was 0.189 ± 0.002 μm^{-2} min^{-1} to fine grains on aluminium disks. Strength (s, in μm^{-2} min^{-1}) was converted to dose rate ($\dot{D}$, in Gymin^{-1}) from ^{241}Am to quartz using Eq. (1), where e is the charge of an electron (in C), S_m is mass stopping power (in MeV cm^2 g^{-1}), and the 10^{17} factor arises from conversion of units (cf. Aitken, 1985a, p. 312).

$$\dot{D} = 10^{17} e \cdot \times S_m \times \cdot s \quad (1)$$

Average α energy delivered in the Littlemore unit was assumed to be 4.2–4.9 MeV (Littlemore, 2001; Singhvi and Aitken, 1978), such that S_m = 675–750 MeV cm^2 g^{-1} for quartz (Zimmerman, 1971, Fig. 5). Average α energy from a 'typical' natural attenuated α spectrum was assumed to be 3.4–3.7 MeV (Zimmerman, 1972; Guerin and Valhadas, 1980; Guerin, 1982), giving a ratio of stopping powers of 0.83. This was used to convert to 'natural equivalent α dose rate to quartz', which was estimated to be 1.89 ± 0.14 Gy min^{-1}. All quoted and plotted α doses are based on this value, to enable direct comparison with β doses and assessment of α efficiency.

β-Induced OSL and TL signals were first studied using prepared 160–250 μm grains from one sample, BZ04. An aliquot was subjected to repeated TL measurement and β irradiation to obtain the natural signal and subsequently sensitise the material in respect of irradiation and heating (Table 1(i)). TL was then measured following irradiation, and preheating and OSL at a range of temperatures. This was to understand signal components present in the sample's TL and OSL in terms of sensitivity to dose, for comparison with commonly observed forms from quartz, and to indicate relationships between them such as: (a) the resistance of TL and OSL signal components to detrapping following different severities of preheat; (b) the sensitivities of TL signals to optical bleaching and hence their potential to produce OSL; (c) the availability of OSL components at different temperatures and hence indications of thermal stability, quenching and/or assistance.

Prepared 160–250 μm grains from sample BZ04 were then investigated in terms of growth in OSL signal in response to α, β, and combined α + β irradiation in the compact crystalline quartz remaining after HF etching (Table 1(ii)). α irradiation would only affect the upper parts of the grains, while β irradiation would affect the whole grains, so β-induced luminescence signals at saturation were expected to be higher than those induced by α irradiation. However, this experiment was designed to evaluate α and β saturation doses, and whether additional signal could be induced by combined α and β irradiation of the same material (i.e. the upper parts of the grains), as experienced in a mixed natural radiation field. Additional aliquots were measured following increasing doses of α and β radiation, until no significant increase was apparent in signal levels normalised to the average of bracketing β dose responses.

Grains (4–11 μm) of milled prepared 160–250 μm grains from sample BZ04 were also investigated in terms of growth in OSL signal in response to α, β, and combined α + β irradiation (Table 1(iii)). This experiment was designed to evaluate saturation doses and signal levels in samples containing enhanced concentrations of structural defects. The 4–11 μm fraction was chosen so that when in a monolayer the whole thickness of the sample material would be subject to α irradiation by the external ^{241}Am source, and so allow calculation of α efficiency values that would be comparable with those obtained from the 'fine grain' fraction in other studies. Additional aliquots were measured following increasing doses of α and β radiation, with the aim of attaining plateaux in signal levels normalised to the average of bracketing β dose responses. This process was terminated at 32 kGyα and 8.4 kGyβ.

The OSL responses of 4–11 μm grains of milled prepared 160 – 250 μm grains from all 34 samples (BZ01-30, BIL01-04) were then measured following irradiations of 113.5 Gyα, 66 Gyβ, and 6.6 Gyβ (Table 1(iv)). This experiment was designed to assess whether the relative α and β responses of the milled material from each sample were similar, and how the α and β responses varied relative to each other with optical stimulation time.

Impurity concentrations in each of the 34 samples were measured using INAA. The milled 200 mg subsamples were packed and sealed into cleaned high-density polyethylene vials, and irradiated for 6 h, in the Portuguese Research Reactor (RPI at ITN, Sacavém) at a thermal flux of 3.96 × 10^{12} n cm^{-2} s^{-1},Φ_{epi}/

Table 1
Luminescence measurement sequences.

	(i) BZ04, 160–250 μm	(ii) BZ04, 160–250 μm	(iii) BZ04 4–11 μm	(iv) BZ01-30, BIL01-04, 4–11 μm
1	TL (500 °C at 5 °C s^{-1})	TL (500 °C at 5 °C s^{-1})	TL (500 °C at 5 °C s^{-1})	TL (500 °C at 5 °C s^{-1})
2	Dose (415 Gyβ)	Dose (83 Gyβ)	Dose (66 Gyβ)	Dose (66 Gyβ)
3	TL (500 °C at 5 °C s^{-1})	PH (260 °C for 30 s)	PH (260 °C for 30 s)	PH (260 °C for 30 s)
4	Repeat steps 2 and 3 to sensitise	OSL (10% LED power, MT = 125 °C)	OSL (10% LED power, MT = 125 °C)	OSL (10% LED power, MT = 125 °C)
5	Dose (415 Gyβ)	TL (500 °C at 5 °C s^{-1})	TL (500 °C at 5 °C s^{-1})	Dose (6.6 Gyβ)
6	PH (40 °C for 30 s)	Repeat steps 2–5 for step 2.	Repeat steps 2–5 for step 2.	PH (260 °C for 30 s)
7	OSL (125 s, 60% LED power, MT = PH − 20 °C)	Dose = α + β, 83 Gyβ. α + β combinations: α to upper grain surfaces ~0, 0.5, 1, 2, 4, 8 kGyα. β: 0, 21, 42, 83, 166 Gyβ	Dose = α + β, 66 Gyβ. α + β combinations: α and α + 0.26 kGyβ: 0, 0.5, 1, 2, 4, 8, 16, 32 kGyα. β: 0.033, 0.066, 0.13, 0.26, 0.5, 1.1, 2.1, 4.2, 8.4 kGyβ	OSL (10% LED power, MT = 125 °C)
8	TL (500 °C at 5 °C s^{-1})			TL (500 °C at 5 °C s^{-1})
9	Repeat steps 5–8 for PH = 80, 120, 160, 200, 240, 280, 320, 360, 400, 440 °C			Repeat steps 2–8 for step 2. Dose = 113.5 Gyα, 66 Gyβ

TL, thermoluminescence; OSL, optically stimulated luminescence; PH, preheat; MT, measurement temperature.

$\Phi_{th} = 1.03\%$, $\Phi_{th}/\Phi_{fast} = 29.77$. Two standards (source of these GSD9, GSS1) were irradiated in an identical geometry for calibration (reference values from Govindaraju, 1994). The samples and standards were analysed by high resolution gamma spectrometry following Prudêncio et al. (1986), Gouveia et al. (1992) and Dias and Prudêncio (2007). Two γ-ray spectrometers were used: a 150 cm^3 coaxial Ge detector (FWHM of 1.9 keV at 1.33 MeV) and a low energy photon detector (LEPD, FWHM of 300 eV at 5.9 keV, 550 eV at 122 keV), both with Canberra 2020 amplifiers and Accuspec B MCAs. The long irradiation permitted quantification of the following elements: Na, K, Fe, Sc, Cr, Co, Zn, Ga, As, Br, Rb, Zr, Sb, Cs, Ba, La, Ce, Nd, Sm, Eu, Tb, Yb, Lu, Hf, Ta, W, Th and U.

In addition to optical examination of prepared but unmilled grains of all samples, backscattered electron images and small area elemental analyses were obtained for sample BZ04. Analysis was conducted at the Laboratório de Caracterização de Materiais, INETI using a Phillips XL30 FEG SEM with XRF attachment. Uncoated grains were mounted on conductive carbon tape, and an accelerator voltage of 5 kV was used to reduce charging.

3. Results

3.1. Microscopy and geochemical analysis

Optical examination indicated the presence of few (approximately one in 50) or very few (approximately one in 200) lightly coloured translucent grains in 16 samples out of the 34. These were considered to be varieties of quartz (e.g. citrine, rose-, smoky-). Also observed were occasional massive or crystalline inclusions (very few for five samples out of the 34). More common were grains containing reddish veins interpreted as iron oxide, and these were seen in a few or very few grains in 25 samples out of the 34. Optical microscopy indicated 'few ferruginous grains' in sample BZ04, but backscattered electron images of the same material showed that roughly one in 20 grains contained higher Z material (Fig. 1a), and a composition indicative of titanite was identified by XRF. More commonly observed were smaller, iron rich inclusions in shallow etch pits (~10 μm across), Fig. 1b), following structural features on the surfaces of more compact grains: lattice boundaries or weaknesses. The depths of etch pits in less compact grains inhibited their examination.

Of the elements analysed for using INAA, Zr and Fe had the higher concentrations (Table 2). Principal components analysis was applied to standardised values of chemical contents, so the analysis was carried out via the correlation matrix. Two-dimensional plots of the factor coordinates were produced for both variables and cases. Fig. 2 presents the projection of the cases; the first factor was extracted to capture the variance to the maximum extent (25.69%) and what remains was recovered by another (second) factor (14.96%), etc.

Standardised values were computed as: Std. score = (raw score − mean)/standard deviation. PCA indicated relationships between Fe, K, Th, U, Cs, and Sm; and between Zr, Hf, Ce, and Ga (henceforth referred to as the Fe and Zr groups). Comparing

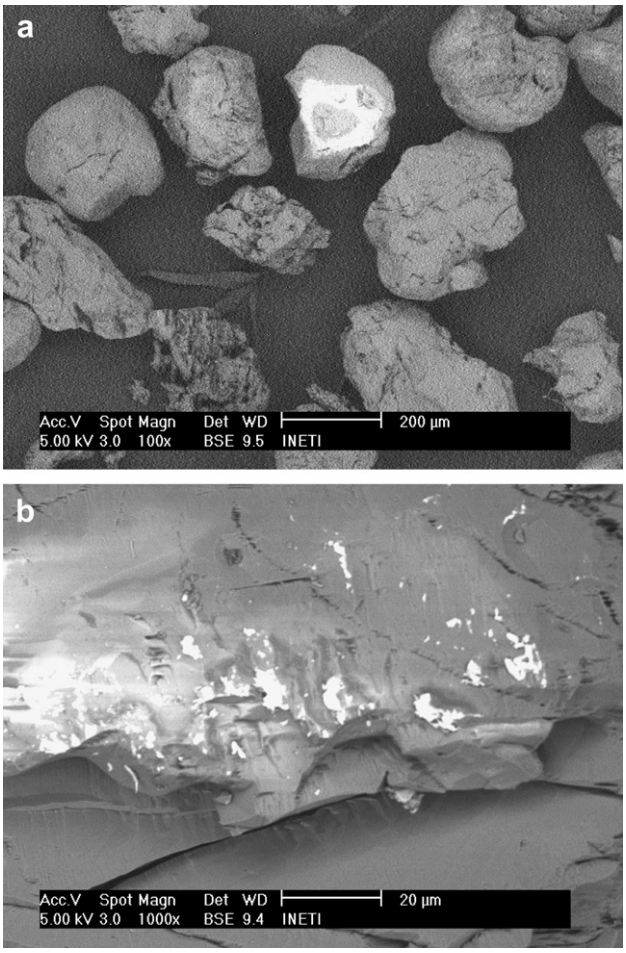

Fig. 1. Backscattered electron images of prepared 160–250 μm grains from sample BZ04. (a) Variety of quartz grains (rounded to subangular, compact to heavily etched), including one with a large high Z inclusion. (b) Higher magnification image of smaller high Z (iron oxide) inclusions in small etch pits at the surface of a compact quartz grain.

Table 2
Elemental concentrations of selected impurities in the prepared quartz in order of concentration, averaged across all samples ($n = 34$).

Element	Concentration	
	Mean (ppm)	SD (%)
Zr	622	18
Fe	96	26
Na	52	34
K	34	33
Th	0.31	20
U	0.14	27

concentrations of each element in the Zr group against Zr yielded r^2 values in the range of 0.88 and 0.99, r^2 for those of the Fe group ranged from 0.15 to 0.43.

3.2. Luminescence analyses

TL from sample BZ04 exhibited peaks at 90, 150, 180, 250, 300, and 350 °C (Fig. 3). The TL intensity in the temperature region 150–300 °C was ~100 cts s^{-1} Gy^{-1}. Stimulation with blue light (125 s at 60% LED power) removed >30% of TL signal in this region, and ~56% around 250 °C. Natural TL was highest around 250–300 °C. TL signals between 350 and 450 °C were reduced very little by blue stimulation, indicating that OSL signals focussed on the 325 °C region, and hence the desired source of OSL signal from quartz could be best isolated by using a preheat 260 °C for 30 s.

Initial OSL signals were very high at lower measurement temperatures (Fig. 3): aliquot size and LED power were reduced for subsequent measurements (Table 1). Initial signals reduced with measurement temperature above 140 °C, while initial decay rate was highest between 140 and 220 °C. The proportion of more slowly decaying signal components, relative to initial signal levels, also varied with measurement temperature. At 20 °C a component was evident between 2.5 and 25 s and is assumed to relate to charge transfer through the trap responsible for the 110 °C TL peak. A different component was evident >25 s at 60 °C but decayed more quickly as temperature increased, such that it was evident between 2.5 and 25 s at 220 °C. A non- or very slowly decaying component was increasingly evident at measurement temperatures of 260 °C and above.

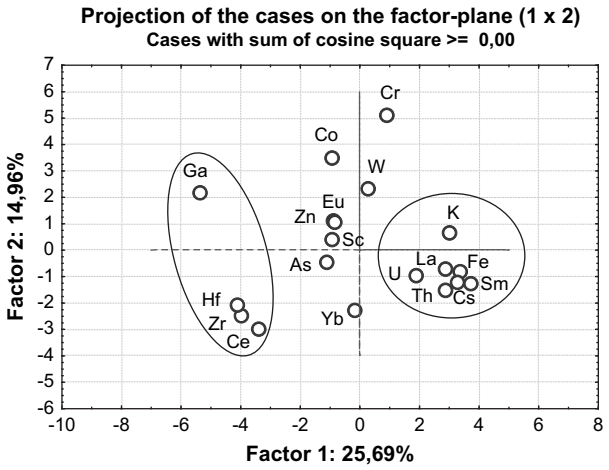

Fig. 2. Principal components analysis of INAA results for prepared 160–250 μm grains that were subsequently milled: components 1 and 2 (41%). Ellipses have been used to highlight observed groupings of elements, but are not the result of statistical analysis. Zr group: Zr, Hf, Ce, Ga, 'Zircon', interpreted as substitutional. Fe group: Fe, K, Th, U, Cs, Sm, 'Iron', interpreted as structural.

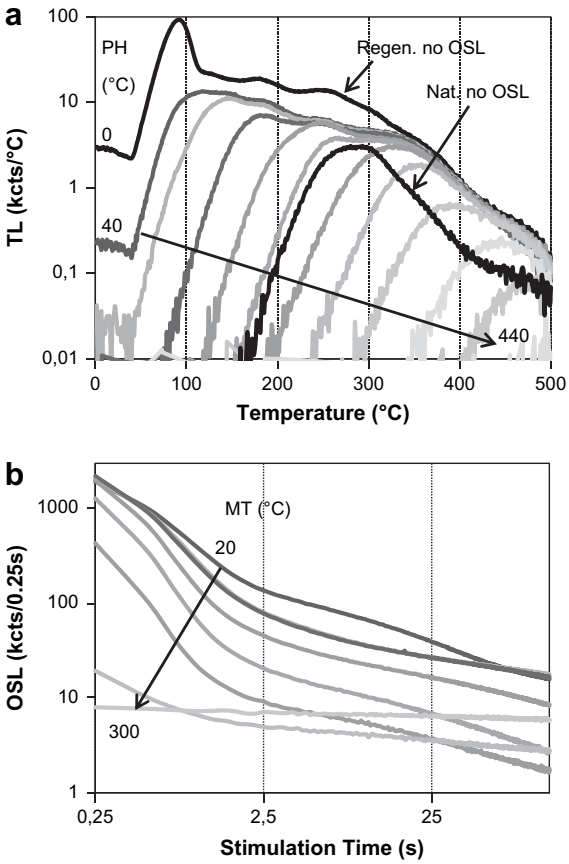

Fig. 3. Sample BZ04, prepared 160–250 μm grains. (a) TL: natural and following regenerative β irradiation, a range of preheats (40 °C steps), and OSL (Table 1(i)). (b) OSL measured at a range of temperatures (40 °C steps; curves for MT = 60 and 100 °C are almost identical).

OSL from β irradiated etched grains increased to approximately 1.5 times the average response to normalisation doses of 83 Gyβ (Fig. 4a). Scatter between the dose-normalised results from different aliquots defined the overall significance of any observed increases, and indicated that the β-induced signals were saturated in the range 166–332 Gy. For no or low β doses, α irradiation of the upper parts of the grains produced significant growth in signal levels to around 4 kGy. Additional signal growth, relative to β-only irradiation, was not induced by α irradiation of the upper parts of the grains. The saturation doses of the β and α responses indicate an α-efficiency (k_{eff}) at saturation of 0.04–0.08. Sensitivity change through the αβ cycle was commonly 0–30%, and no α or β dose dependence was evident (Fig. 4b).

OSL responses of 4–11 μm grains of prepared milled material to α, β, and α + β radiation, normalised to responses to bracketing β doses of 66 Gy, exhibited continuing growth to 32 kGyα and 8.4 kGyβ, and signal levels over 20 times the average response to the normalisation doses (Fig. 5a). Signal matching α and β responses indicated α efficiencies (k_{eff}) of ~0.13 at lower doses, increasing with dose to greater than 0.25. Sensitivity to the normalisation dose commonly increased by 1.4 to 2 times through the αβ cycle, but did not differ consistently between α and β irradiation, nor vary consistently with dose (Fig. 5b).

Estimates of the relative OSL response of 4–11 μm milled grains to relatively low α and β doses (Table 1(iv)) were similar across the 34 samples, but varied strongly with stimulation time: $\mu_{keff} \pm \sigma_{keff}$

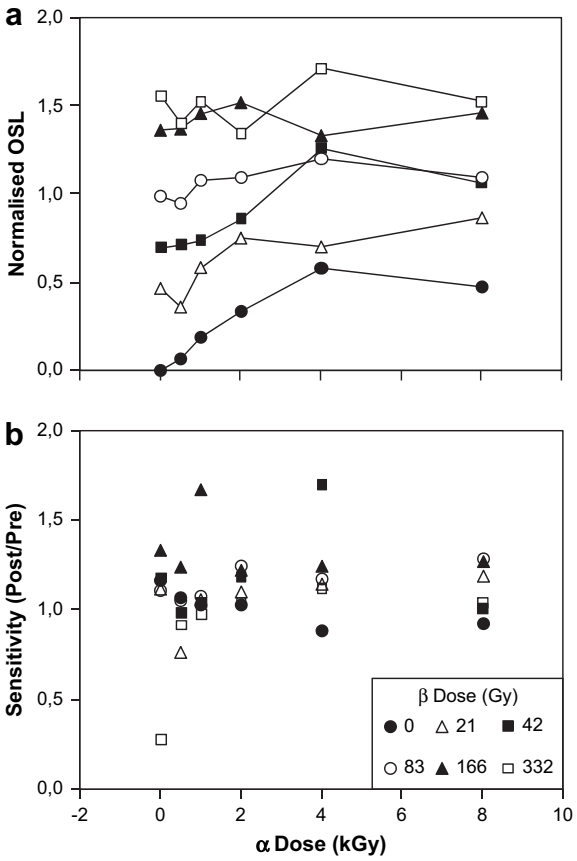

Fig. 4. Sample BZ04, 160–250 μm grains. (a) OSL signal response to different combinations of α and β dose (Table 1(ii)), normalised to the average OSL response to bracketing β doses. (b) Sensitivity change: ratio of β sensitivity before and after the αβ cycle.

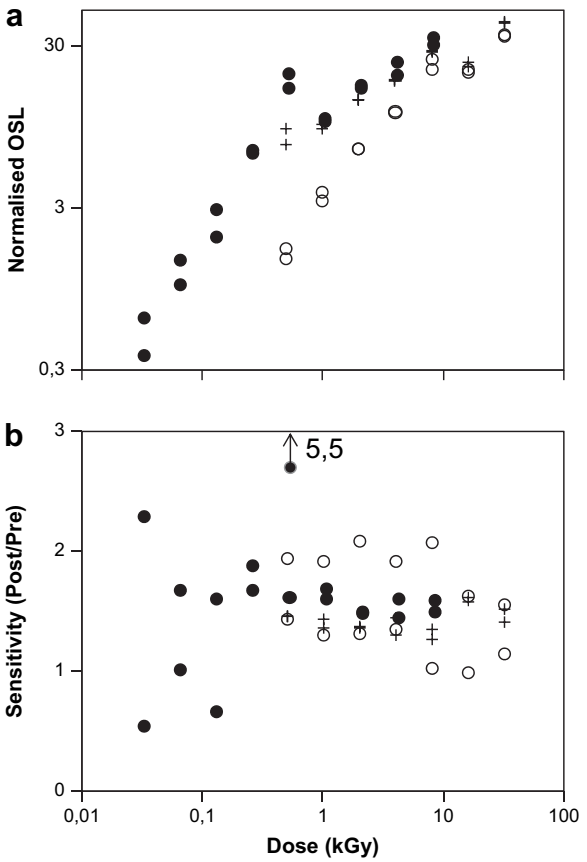

Fig. 5. Sample BZ04, 4–11 μm milled grains. (a) OSL signal response to different combinations of α and β dose (Table 1(iii)), normalised to the average OSL response to bracketing β doses. (b) Sensitivity change: ratio of β sensitivity before and after the αβ cycle. Closed circles, β irradiation only; open circles, α irradiation only; crosshairs, α + 264 Gy β.

for integrals of 0–0.5 and 0–50 s were 0.11 ± 0.03 and 0.34 ± 0.07 respectively. Two signal components were evident in the OSL decay curves (Fig. 6). The initial OSL signal induced by α irradiation was close to that induced by the lower β dose (low k_{eff}), but the α response of the slower component was closer to that of the higher β dose (high k_{eff}). As a proportion of initial signal, the slower component was smallest following the lowest β dose, larger for the higher β dose, and largest for the α dose.

4. Discussion

The increase in k_{eff} with dose observed in the milled material is consistent with earlier onset of saturation in the β response than that to α radiation. Their growth characteristics appear similar to a combination of Zimmerman's (1972, Fig. 9) results for the 110 and 300 °C TL peaks, for which k_{eff} values of 0.018 and 0.1 were determined at 'saturation' β doses. Mauz et al. (2006) determined *a*-values for OSL of silt sized quartz of ~0.03 using β doses in the 'linear' region, and ~0.1 for β doses around 200 Gy (k_{eff} ~0.036 and ~0.12). The k_{eff} values measured on milled material in the present study were higher (0.13–0.34), but the estimate of 0.04–0.08 at saturation for the clean, compact and crystalline upper parts of the coarse grains is similar. This value is not subject to geometric correction (Aitken, 1985b, Eq.7), since it is based on saturation dose for each signal (166–332 Gyβ, ~4 kGyα, Fig. 4) rather than comparison of induced signal levels. Higher α efficiency in the milled material is likely to result from high defect concentrations, which are able to trap a greater proportion of the energy deposited along each α track.

Variations in k_{eff} with stimulation time in the milled material indicated changing contributions from OSL components with different properties (Fig. 6): a more optically sensitive trap with a higher specific trapping cross section, and a less optically sensitive

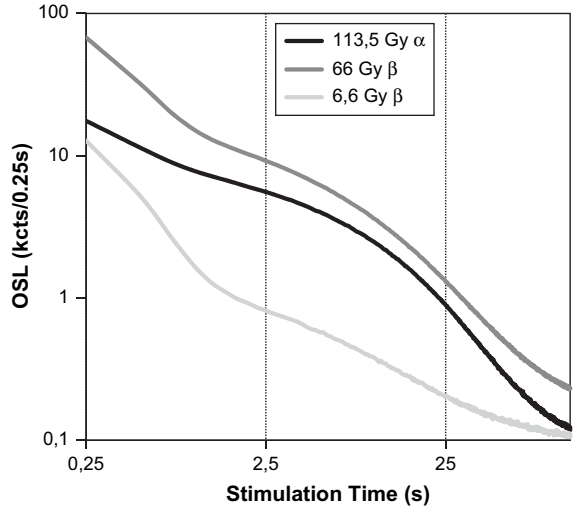

Fig. 6. OSL decay curves measured following α and β irradiation of 4–11 μm milled grains (Table 1(iv)). Average signal from 34 aliquots: one aliquot from each of 34 samples.

trap with a lower one (slower decaying component). Of the much less prominent slower components observed in the unmilled material (Fig. 3b), the second component of the three described in Section 3.2 had a similar lifetime to that of the milled material (taking into account the difference in stimulation intensity: 10% vs. 60% LED power, Table 1). This may be a 'medium' component of quartz (e.g. Singarayer and Bailey, 2003), and the present study indicates that it may relate to naturally present structural defects. Variations in such defect concentrations might help explain some different types of dose response seen in OSL measurements of 'quartz'.

SEM analysis combined with XRF showed that Fe was present along weaknesses close to the surfaces of compact coarse grains: at the bottom of etch pits (Fig. 1). Principal components analysis of INAA results associated the Fe with a group of elements not likely to be mineralogically associated, including K, U and Th (Fig. 2). Optical microscopy indicated reddish veins of weakness running through some grains, and hence that the Fe (with K, U, and Th, among others) has accumulated in and along existing voids and structural weaknesses in the crystal. This may have occurred by coprecipitation from solution or coinfiltration, during the process of the grains accumulating the exterior coatings common in arid environments (Watchman, 2000). Such voids or weaknesses in the crystals may be regarded as internal or internalised surfaces, with associated structural defects in the crystal around. Some grains observed by SEM were highly pitted following HF treatment, such that most of the internal surfaces are thought to have been etched away. In more compact grains, however, where such voids/weaknesses were perhaps smaller, the HF did not penetrate sufficiently to dissolve their contents (Fig. 1). Relatively high levels of Zr were also measured by INAA, and associated with other elements found in zircon (Fig. 2), but not with U or Th. Titanite was also identified, by XRF. Both impurities and structural defects in the quartz may therefore have contributed to the broad distribution of TL peaks observed from sample BZ04 (Fig. 3). However, preheating to 260 °C for 30 s was sufficient to remove the majority of optically sensitive TL that may have derived from these.

Average U and Th concentrations determined by INAA (Table 2) are similar to those from the majority of samples reported by Mejdahl (1987). If evenly distributed they would produce an infinite matrix α dose rate of 0.6 mGy a^{-1}. Previous studies have regarded this estimate as an upper limit due to expected inhomogeneity (e.g. Vandenberghe et al., 2008). The present data indicated that α activity was highly localised, so the fraction of the bulk quartz that would have received α radiation from Th and U in inclusions of a range of diameters was estimated, using Eq. (2) and the average concentrations in Table 2.

$$F_\alpha = C_{\text{inc.}}(\rho_{\text{inc}}/\rho_{\text{Qtz}}) \cdot ((R_\alpha + r_{\text{inc}})/r_{\text{inc}})^3 \quad (2)$$

where F_α is the α irradiated fraction, C_{inc} is the fractional concentration of inclusion mineral, ρ is the mineral density (inclusion, quartz), R_α is the α range in quartz, r_{inc} is the inclusion radius.

This was designed to evaluate the effect of inclusion 'scale' and assumed evenly distributed spherical inclusions: uneven distribution would increase the effective scale. Other assumptions and approximations were: average α energy 3.4–3.7 MeV, and hence range in quartz ($\rho = 2.625$ g cm^{-3}) = 11.4 μm (from Brennan and Lyons, 1989); α activity (Th, U) only present in inclusions of the type calculated for; Zr in crystalline $ZrSiO_4$, $\rho = 4.7$ g cm^{-3}; Fe in massive Fe_2O_3, $\rho = 5$ g cm^{-3}; Na, K present as Na_2O, K_2O in crystalline feldspathic material, $\rho = 2.6$ g cm^{-3}.

The curves in Fig. 7 indicate that given the size (~10 μm) and distribution of Fe inclusions identified by SEM, internal α radiation affected less than 1% of the bulk quartz.

OSL from the bulk quartz saturated by 332 Gyβ and 4 kGyα (coarse grains, Fig. 4a), and achieved normalised signal levels of ~130 Gy (normalisation dose × normalised signal ratio). The responses of the milled material exhibited a degree of saturation, but continued to grow strongly at 8.4 kGyβ and 32 kGyα (Fig. 5a), where normalised signal levels were in excess of ~1300 Gy. Even for a single signal component or material type, use of a non-linear β or γ growth curve to calibrate a natural signal with a significant α contribution will produce a substantial age overestimate (Aitken, 1984). In the present case, the signal able to grow to high doses and signal levels also had a high α efficiency and spatially associated source of α radiation. Such a signal would exhibit continued growth to high doses in the laboratory, but in nature would represent a very much larger absorbed dose than the signal from the crystalline quartz. It would therefore contribute a larger proportion of the combined natural signals than of the combined signals induced by β irradiation. Differences in this proportion as a function of stimulation time would produce variations in equivalent dose. Accurate age estimation in this situation would require knowledge of the proportions and of the dosimetries relating to each signal. Further, if its relative contribution to the combined signals induced by β irradiation were low and the α dose absorbed in nature high, then the natural signal would appear to lie above the signal saturation level attainable in the laboratory: achieving this level would be subject to second order effects of high dose irradiation of the crystalline material.

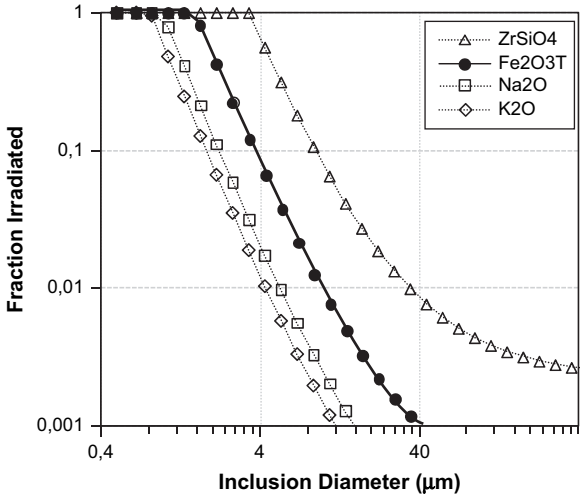

Fig. 7. Fraction of prepared quartz reached by internal α radiation for a range of inclusion scales, calculated using Eq. (1) using the concentrations listed in Table 2.

The effect of such signal components will be lowest while the signal of interest from the bulk quartz grows strongly with dose. However, ideally such signals would be isolated or avoided. U, Th and hence any such effects, have been related to the presence of Fe in these samples, and since optical examination indicated that a proportion of grains contained iron oxide, it would be logical to attempt to remove these grains using magnetic separation (Porat, 2006). Alternative approaches might involve separation of OSL signal components, and rejection of grains based on single grain component analysis and/or microscopy of single grains after luminescence measurement.

5. Conclusions

Impurities including a range of elements in structural defects, and substantial zircon and titanite inclusions, may remain in quartz grains after conventional preparation procedures for luminescence measurements. Examination of TL response may serve to indicate both their presence and an appropriate preheating regime for OSL measurements. In the present suite of samples U and Th, and hence

internal α activity, were spatially associated with the presence of Fe, which was identified along structural defects in these quartz crystals. This is considered to indicate codeposition of U and Th with Fe along weaknesses within the coarse grains, which was not removed by etching in hydrofluoric acid, and the potential to remove the most affected grains by magnetic separation. Consideration of the size and concentration of such inclusions indicated that α dose rate to the bulk quartz would be insignificant. However, structural (surface) defects in milled grains were shown to produce OSL signals with high saturation doses and α efficiencies. Signals from similar defects in the internal surfaces of larger grains may contribute to variations in the form of dose response from quartz. α irradiation of such defects by associated impurities would produce overestimates in equivalent dose, and variations in equivalent dose with stimulation time. Saturation levels of natural signals containing such components should be attainable by laboratory irradiation, but could require irradiation of the whole grains to doses considered geologically unreasonable, or subject to changes in the dosimetric behaviour of the crystalline quartz contributing the majority of the OSL signal.

Acknowledgements

The authors wish to thank Engenheira M. Manuela Oliveira and Vanessa Livramento for access and assistance with the SEM analyses. This work forms part of a project co-financed by the Instituto Português de Apoio ao Desenvolvimento, Instituto Nacional de Engenharia Tecnologia e Inovação, Instituto Público, and Direcção Nacional de Geologia (de Moçambique), into the geological development of the Mozambican coastal plain. Attendance at the conference was assisted by a travel grant from the Fundação Calouste Gulbenkian. Thanks also to the reviewer, whose comments greatly improved the manuscript.

References

Aitken, M.J., 1984. Non linear growth: allowance for alpha particle contribution. Ancient TL 2 (1), 2–5.
Aitken, M.J., 1985a. Thermoluminescence Dating. Academic Press, London.
Aitken, M.J., 1985b. Alpha particle effectiveness: numerical relationship between systems. Ancient TL 3 (3), 22–25.
Armitage, S.J. 2003. Testing and application of luminescence techniques using sediment from the southeast African coast. PhD thesis, University of Wales, Aberystwyth.
Armitage, S.J., Botha, G.A., Duller, G.A.T., Wintle, A.G., Rêbelo, L.P., Momade, F.J., 2006. The formation and evolution of the barrier islands of Inhaca and Bazaruto, Mozambique. Geomorphology 82, 295–308.
Bailey, R.M., Armitage, S.J., Stokes, S., 2005. An investigation of pulsed irradiation regeneration of quartz OSL and its implications for the precision and accuracy of optical dating (Paper II). Radiat. Meas 39, 347–359.
Bøtter-Jensen, L., Bulur, E., Duller, G.A.T., Murray, A.S., 2000. Advances in luminescence instrument systems. Radiat. Meas 32, 523–528.
Brennan, B.J., Lyons, R.G., 1989. Ranges of alpha particles in various media. Ancient TL 7, 33–37.
Dias, M.I., Prudêncio, M.I., 2007. Neutron activation analysis of archaeological materials: an overview of the ITN NAA laboratory. Portugal. Archaeometry 49, 383–393.
Gouveia, M.A., Prudêncio, M.I., Morgado, I., Cabral, J.M.P., 1992. New data on the GSJ reference rocks JB-1a and JG-1a by instrumental neutron activation analysis. J. Radioanal. Nucl. Chem. 158, 115–120.
Govindaraju, K., 1994. Compilation of working values and sample description for 383 geostandards. Geostandards Newsletter 18 (special issue), 1–158.
Guerin, G., 1982. Croissance de la thermoluminescence en fonction de la dose des feldspaths d'origene volcanique. PACT 6, 417–425.
Guerin, G., Valhadas, G., 1980. Thermoluminescence dating of volcanic plagioclases. Nature 286, 697–699.
Kibar, R., Garcia-Guinea, J., Çetin, A., Selvi, S., Karal, T., Can, N., 2007. Luminescent, optical and colour properties of natural rose quartz. Radiat. Meas 42, 1610–1617.
Krbetschek, M.R., Gotze, J., Dietrich, A., Trautmann, T., 1997. Spectral information from minerals relevant for luminescence dating. Radiat. Meas 27, 695–748.
Littlemore, 2001. Calibration Report: 6 Source Alpha irradiator #0103311603. Littlemore Scientific Engineering, Oxford, UK.
Mauz, B., Packman, S., Lang, A., 2006. The alpha effectiveness in silt-sized quartz: new data obtained by single and multiple aliquot methods. Ancient TL 24, 47–52.
Mejdahl, V., 1987. Internal radioactivity in quartz and feldspar grains. Ancient TL 5, 10–17.
Mercier, N., Valladas, H., Valladas, G., 1992. Observations on palaeodose determination with burnt flints. Ancient TL 10, 28–32.
Miallier, D., Gibert, F., Fain, J., Pilleyre, T., Sanzelle, S., 2001. Fluid inclusions in quartz: interference with thermoluminescence and its application to dating. Quat. Sci. Rev. 20, 901–905.
Porat, N., 2006. Use of magnetic separation for purifying quartz for luminescence dating. Ancient TL 24, 33–36.
Prudêncio, M.I., Gouveia, M.A., Cabral, J.M.P., 1986. Instrumental neutron activation analysis of two French geochemical reference samples – basalt BR and biotite Mica-Fe. Geostandards Newsletters X, 29–31.
Richter, D., Zink, A., Przegietka, K., Cardoso, G.O., Gouveia, M.A., Prudêncio, M.I., 2003. Source calibrations and blind test results from the new Luminescence Dating Laboratory at the Instituto Tecnológico e Nuclear, Sacavém. Portugal. Ancient TL 21, 1–7.
Singarayer, J.S., Bailey, R.M., 2003. Further investigations of the quartz optically stimulated luminescence components using linear modulation. Radiat. Meas 37, 451–458.
Singhvi, A.K., Aitken, M.J., 1978. Americium-241 for alpha irradiations. Ancient TL 3, 2–9.
Vandenberghe, D., De Corte, F., Buylaert, J.-P., Kucera, K., Van den haute, P., 2008. On the internal radioactivity in quartz. Radiat. Meas 43, 771–775.
Watchman, G., 2000. A review of the history of dating rock varnishes. Earth Sci. Rev. 49 (1-4), 261–277.
Zimmerman, D.W., 1971. Thermoluminescence dating using fine grains from pottery. Archaeometry 13, 29–52.
Zimmerman, D.W., 1972. Relative thermoluminescence effects of alpha- and beta-radiation. Radiat. Eff 14, 81–92.